M S Aboraia, H S Wasly, M A Doheim, G A Abdalla, A E Mahmoud / International Journal of Engineering Research and Applications (IJERA) ISSN: 2248-9622 www.ijera.com
Vol. 3, Issue 3, May-Jun 2013, pp.474-482

Characterization of Al/(10%Al_2O_3-10%ZrO_2)Nanocomposite Powders Fabricated by High-Energy Ball Milling

M S Aboraia[1], H S Wasly[2], M A Doheim[1] , G A Abdalla[1] and A E Mahmoud[1]

1Mining and Metallurgical Engineering Department, Faculty of Engineering, Assiut University, Assiut, Egypt
2Mining and Metallurgical Engineering Department, Faculty of Engineering, Al-Azhar University, Qena, Egypt

Abstract

Al–10% Al_2O_3-10% ZrO_2 nanocomposite powders were fabricated by high-energy milling of the blended component powders. Planetary Monomill "Pulverisette 6" was used in milling the powders for 45 hours at 300 rpm and a ball-to-powder ratio of 10:1. A uniform distribution of the Al_2O_3 and ZrO_2 reinforcements in the Al matrix was successfully obtained after powders milling process. This uniform distribution was confirmed by characterizing these nanocomposite powders by scanning electron microscopy (SEM). X-ray diffraction (XRD) patterns were recorded for the milled powders, and analyzed using Williamson–Hall method to determine the crystallite size and the lattice strain. The crystallite size measurements were obtained using TEM observations in order to compare these results with those obtained from XRD

Keywords: **Al-Al_2O_3-ZrO_2; High-energy milling; Nanocomposites**

I. Introduction

Metal matrix composites have both the metallic properties of ductility and toughness, and the ceramic properties of high strength at elevated temperatures. Aluminum composites have attracted considerable attention in structural and functional applications owing to their light weight and high specific strength [1]. The homogeneous distribution of the fine reinforcement (ceramic) throughout the Al matrix and a fine grain size of the matrix have a great effect in improving the mechanical properties of the composite[2].

High energy ball milling is used as a processing method to fabricate MMCs [3-7]. This process is a powder processing method in which powder particles go through a repeated process of cold welding, fracturing, and rewelding. The continuous interaction between the fracture and welding events tends to refine the grain structure and leads to a uniform distribution of the fine reinforcement particles in the metal matrix [8].

Al matrix can be reinforced with different ceramic particles of different shapes and sizes to achieve the desired properties [9-12]. In this study, both alumina and zirconia were used as the reinforcement material for Al matrix. Alumina used, because it is chemically inert with Al, and also can be used at elevated temperatures [7]. Zirconia is also one of the most important ceramic materials, due to its excellent mechanical properties like flexural strength and fracture toughness, which makes it also suitable for its use in ceramic engines and in many other ceramic components in industrially severe conditions as wear applications [13].

The aim of the present investigation is to synthesize and characterize aluminum reinforced with a uniform dispersion of specified weight fraction nanometer-sized alumina and zirconia particles, starting from micron size. The alumina-zirconia system is presented as a model system to create advanced material of Al-Al_2O_3-ZrO_2 hybrid nanocomposite with new properties.

II. Experimental Work

2.1 Materials

The materials used in the experiments were Commercial aluminum powder with a particle size of (-210 + 90 μm) , Commercial alumina powder with particle size smaller than 44 μm and zirconia powder with particle size smaller than 38 μm. Scanning Electron Microscope (SEM) analysis using a JEOL-JSM 5400F for the powders is given in Fig. 1. Fig. 1(a) shows that Al particles are irregular in shape and alumina particles in Fig. 1(b) are almost spherical. It can be seen from Fig. 1(c) that zirconia powders tend to form conglomerates of particles.

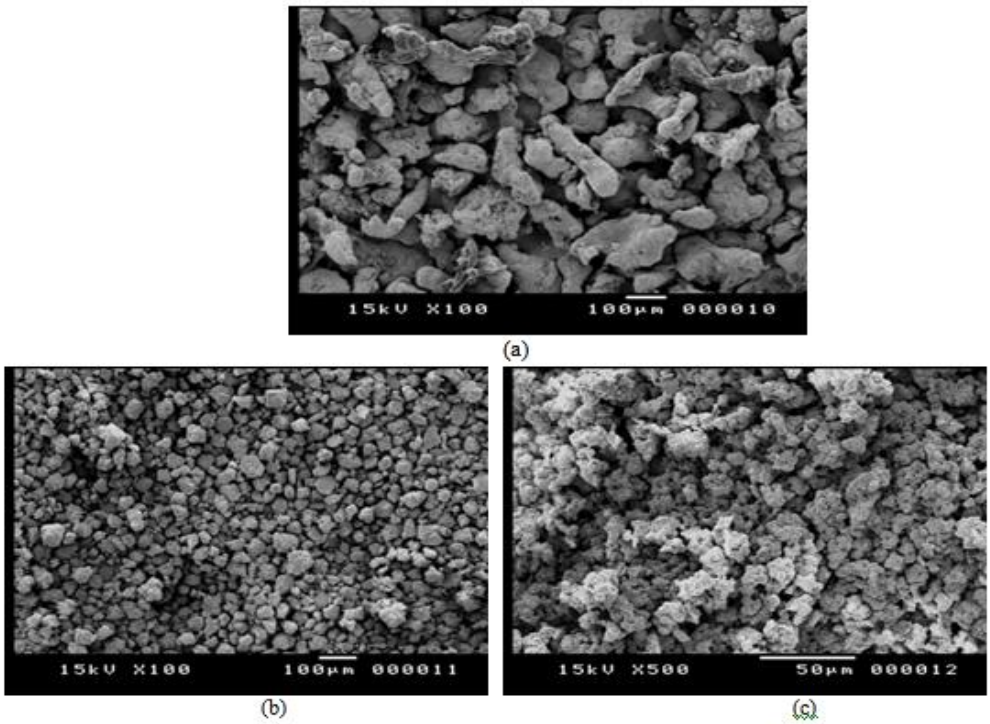

Fig. 1: SEM images for the as-received powders: (a) Aluminum (b) Alumina (c) Zirconia

2.2. Milling of powders

Planetary Monomill "Pulverisette 6" was used for the mechanical milling of the powders mixture. Grinding is carried out under Argon gas atmosphere at 300 rpm milling rotation speed and ball-to-powder ratio of 10:1. Stearic acid was used as a process control agent (PCA) to prevent the aggregation of powders during milling. The duration of milling process is fixed at 30 min at a time in order to avoid temperature rise and the samples were taken at different periods of time at 7, 12, 15, 21, 30, 38 and 45 hours.

2.3 Structural Analysis and Characterization

X-ray diffraction patterns were recorded for the as-received and milled powders using a Philips PW 1710 X-ray diffractometer using Cu Kα radiation (λ = 0.15406 nm) at 40 kV and 30 mA settings. The XRD patterns were recorded in the 2θ range of 20°–90°. The changes of peak shape, during the powder milling process, are related to microstructural changes. The experimental line broadening may be related to three contributions, which are the crystallite sizes, lattice strains and the instrumental effects [14]. There are techniques, such as the Williamson–Hall [15] and Halder–Wagner methods [14], used to determine the grain size and the equivalent strain.

In the Williamson–Hall (WH) treatment, the full width at half maximum (FWHM), β, due to sample imperfections is related to the crystallite size, *D*, and the distortions, ε, by the equation:

$$\beta^* = d^*\varepsilon + 1/D \quad \ldots\ldots\ldots\ldots\ldots\ldots\ldots\ldots\ldots (1)$$

Where $\beta^* = \beta \cos\theta / \lambda$ and $d^* = 2\sin\theta/\lambda$; θ is the Bragg angle and λ is the used X-ray wavelength (λ = 0.15406 nm). The experimental breadth of a given reflection was fitted for the peak breadth from the instrument by Voigt functions using the Originpro 8 software. FWHM is corrected, using silicon as standard reference material. values of β^* and d^* can be calculated correctly from the previous equations. Then from plotting β^* against d^* crystallite size and strain can be obtained where, the intercept of the plot of β^* against d^* gives $1/D$ and the slope gives the strain [16].

2.4 Microstructural characterization

After milling, the powders were characterized for their microstructure and distribution of Al_2O_3&ZrO_2 particles in the Al matrix using a JEOL-JSM 5400 F scanning electron microscope (SEM). Energy dispersive X-ray analysis (EDS) of the powders mix, without milling, and the as-milled powders was applied for compositional analysis. The microstructure was observed by transmission electron microscopes (TEM) using Joel JEM–100CXII. Direct TEM observations used in measuring the crystallite size and the results are compared with the results obtained from Williamson–Hall method.

III. Results and Discussion

3.1 X-ray diffraction analysis

Fig. 2 shows the X-ray diffraction patterns of the Al–10%Al_2O_3-10%ZrO_2 powders milled with rotation speed 300 rpm at different periods of time (7, 12, 15,

21, 30, 38 and 45 hours). It can be seen that line broadening increases with milling time. Due to high energy milling which involves repeated deformation, cold welding, and fragmentation, structural changes such as decrease in crystallite size, accumulation of microstrain, and dislocations occur in deformed powder. So, the X-ray line broadening analysis has been used to characterize the microstructure in terms of crystallite size and lattice strain. Line profile analysis confirmed the evolution of the apparent size, D, and the equivalent lattice strain, ε, with milling time [2,17]. The profiles of all Bragg reflections are broadened; this is related to the reduction of crystallite size and to the important lattice strain introduced by milling.

The broadening increases with milling time in XRD pattern and can be shown clearly with plotting single peak lines of Al–Al_2O_3-ZrO_2 powders milled for different times. Fig. 3 shows profiles plotting for only the first peak (P1), of the milled powders for different times. It's noted that with milling time, peak broadening increases and the peak is shifted to higher θ values. The change of the lattice parameter during milling is probably one of the reasons of this shift which was observed by others [18, 19].

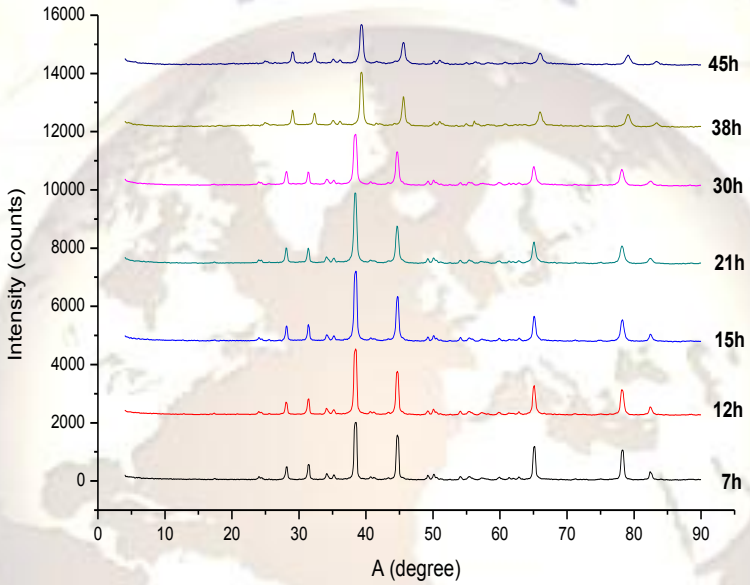

Fig. 2: XRD patterns of Al–Al_2O_3-ZrO_2 powders milled for different times; 7, 12, 15, 21, 30, 38 and 45 h.

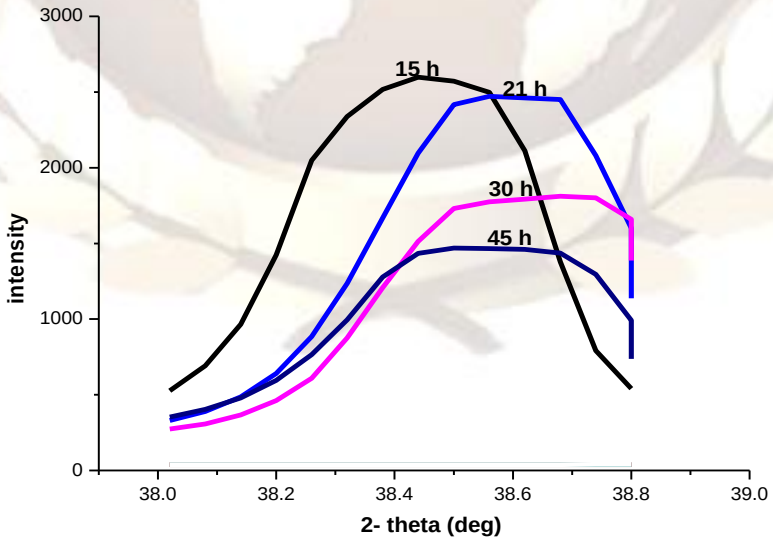

Fig. 3 : Bragg reflections Profiles of the first peak- of milled Al–Al_2O_3-ZrO_2 composites powders for different times (15, 21, 30, 45 hours).

By using the previous equations; $\beta^* = \beta \cos\theta / \lambda$ and $d^* = 2 \sin\theta/\lambda$; values of β^* and d^* can be calculated. From Plotting β^* against d^*, the crystallite size *D*, and the lattice strain ε of composites at different times are obtained. Where, the curve intercept gives 1/*D* and the slope gives the strain. Al D and ε values for different samples (7, 12, 15, 21, 30, 38 and 45 hours) of the Al–Al_2O_3-ZrO_2 nanocomposite are obtained and plotted in Fig. 4 . Fig. 4 shows the variation of the crystallite size and of the lattice strain against milling time obtained by Williamson–Hall method, for Al–Al_2O_3-ZrO_2 powders milled at 300 rpm. It can be seen that the rate of the grain refinement continuously decreases reaching, after 45h of milling, the value of 25.36 nm. While, the lattice strain shows a continuous increase to a value of 0.139%. From Fig.4 , It's noted that the milling induces a higher lattice strain and an evolution of the finest particles, mainly in the extended times of milling. The low crystallite size can be related to the action between the levels of stress produced by a milling device, and the degree of dynamic recovery in the milled material [17, 18].

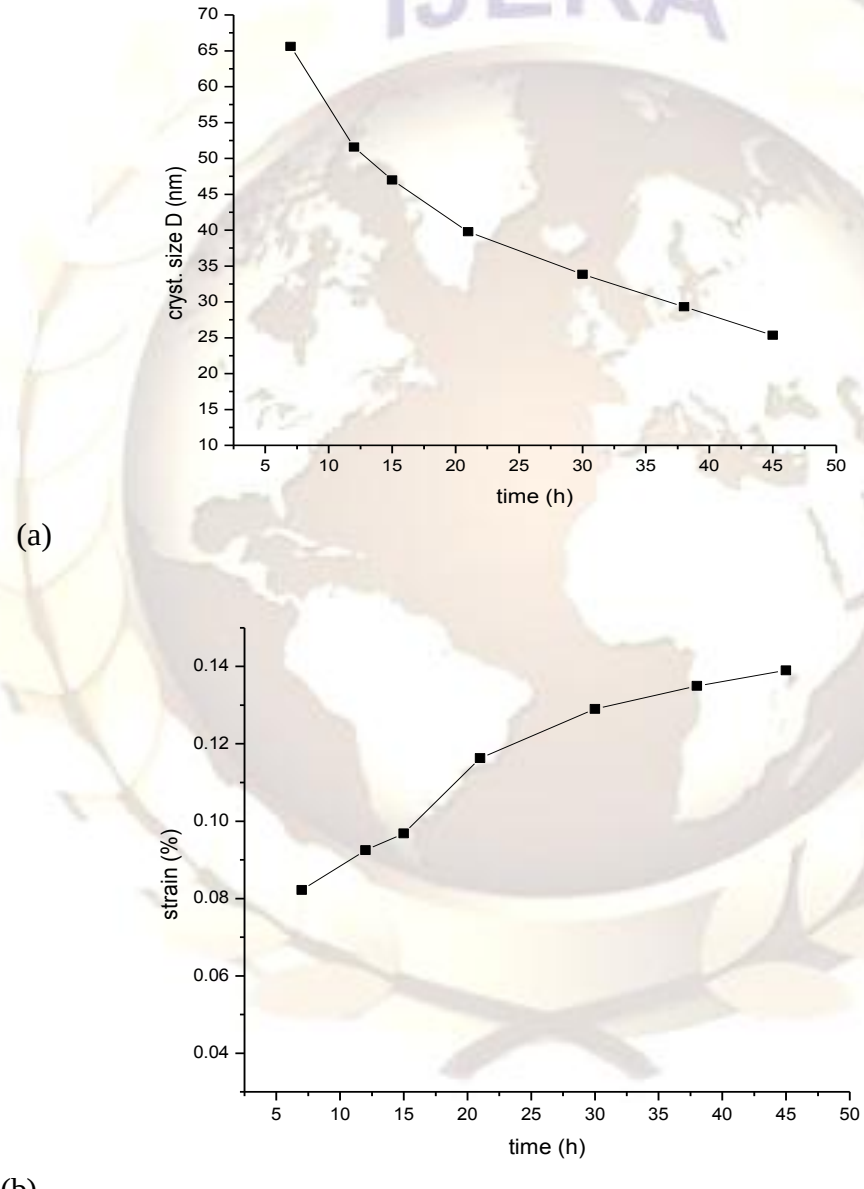

Fig. 4: Changes of crystallite size and lattice strain of the milled Al–Al_2O_3-ZrO_2 powders as a function of milling time (a) crystallite size (b) lattice strain .

3.2. Microstructural observations

The main objective of the investigation was to ensure that a homogeneous distribution of Al_2O_3& ZrO_2 in Al matrix was achieved after milling. The uniform distribution of reinforcements could potentially result in composites with improved mechanical properties. Fig. 5 shows the SEM images of Al–Al_2O_3-ZrO_2 powder particles at different milling times for 300 rpm milling speed. As expected at initial milling time the reinforcement particles distribution was not uniform and they are far from each other. But, increasing milling time causes breakage of the big and brittle reinforcement powders. With continued milling the powder particle size decreased due to the predominance of the fracturing of powder particles over the cold welding process. At 7h milling Fig. 5 (a), particles have been under deformation and cold welding therefore, flattened particles were formed. This is because aluminum particles are soft and their sizes increased by cold welding. The rate of fracturing tends to increase with increasing milling time. The fragmentation of the flattened particles was detected and equiaxed particles are formed after 15h of milling, Fig. 5 (b).

At 30h milling time Fig. 5 (c), because of work hardening of the soft aluminum powders, along with cold welding of the particles, fragmentation was happened in a large amount and particle size decreased. Also, alumina and zirconia reinforcement particles have been moved in welded aluminum and confined between them. At 45h milling time, Fig. 5 (d), because the particles work hardened and become brittle, so the fracturing rate of the particles increases and the particles size decreases. The larger particles at Fig. 5 (d) appeared to be agglomerates of many smaller particles and at longer milling times the powder particles were more uniform in size compared to the early stages of milling. These SEM results of powder particles at different milling times are generally in agreement with those observed by others [2,7,20] for a different system (Aluminum-alumina powder).

Milling of Al–10%Al_2O_3-10%ZrO_2 powders-300rpm extended to 45 hours. It is important to know that the uniform distribution of alumina and zirconia reinforcements in Al matrix begins early as observed from SEM images (Fig. 5). But milling continued till 45 hours in order to reach to nanosize for the particles as much as possible, especially the milled particles starting from micron size. And the dominant reason for stopping milling is the diffraction pattern for the different samples and peaks broadening. At 45h milling, fine particle size leads to broadening of the peaks and it is difficult to find sharp peaks in the diffraction pattern, consequently the height of the peaks is smaller.

3.3 EDS Analysis

EDS analysis of the Al–10% Al_2O_3-10% ZrO_2 mix without milling and the as-milled powders showed that contamination is found in the milled powder as a result of the high energy milling process. The factors contributing to the powder contamination increase; small size of the powder particles, availability of large surface area, and new fresh surfaces formation during milling. Fig. 6 shows the EDS spectra for the Al–Al_2O_3-ZrO_2 mix without milling and the as-milled Al–Al_2O_3-ZrO_2 powders milled at 300 rpm for 45 h. It can be seen from the peaks present in the as-milled Al–Al_2O_3-ZrO_2 spectrum a presence of additional elements due to contamination from the milling media. Contamination (e.g. Fe) has been found to be normally present in most of the powders milled with steel grinding medium [21].

a)

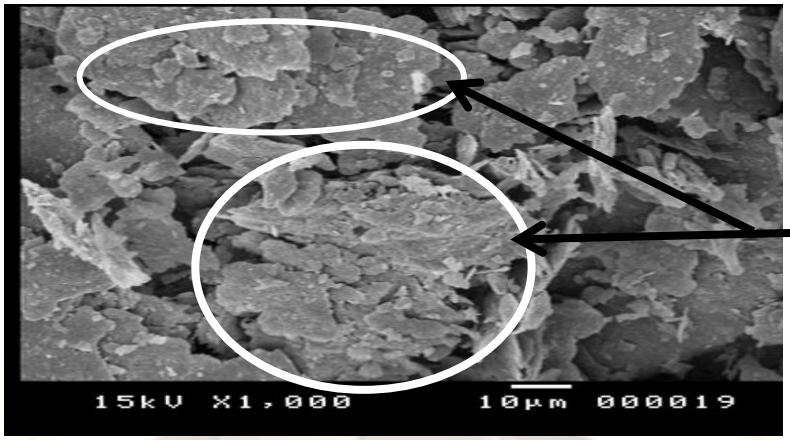

Flattened Al

b)

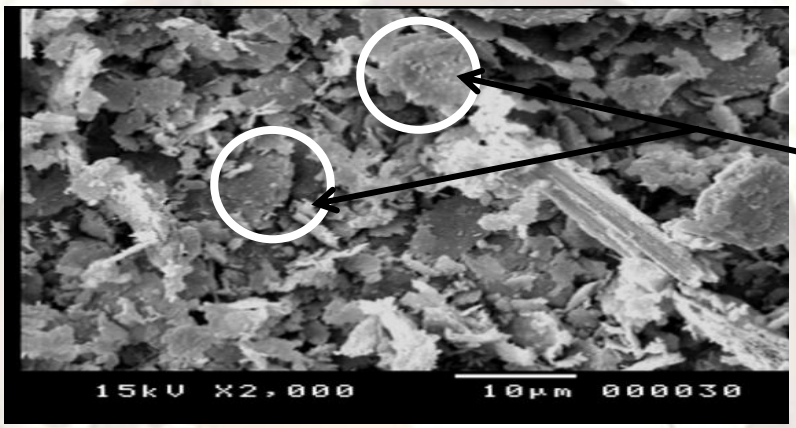

equiaxed Al particles

c)

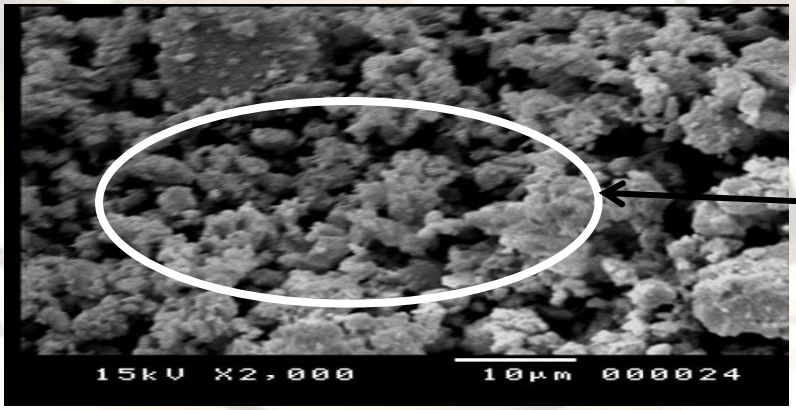

Al particles decreased & Al_2O_3confined between them

d)

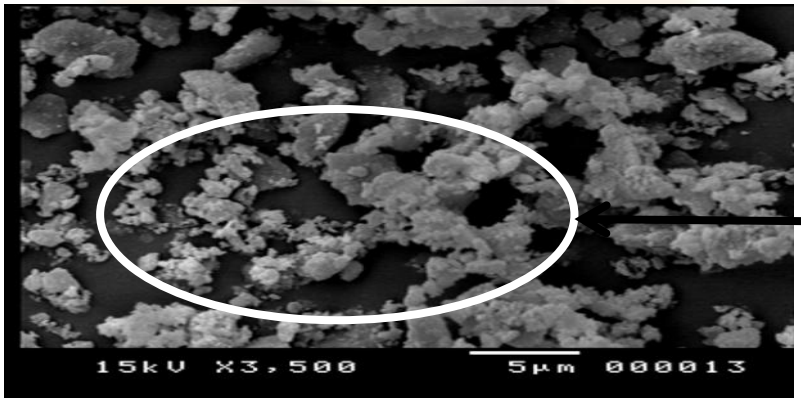

Particles size decreased & the powder become more uniform

Fig. 5: SEM micrographs of milled Al–Al_2O_3-ZrO_2 powder particles at different milling times: (a) 7h, (b) 15h, (c) 30h (d) 45h

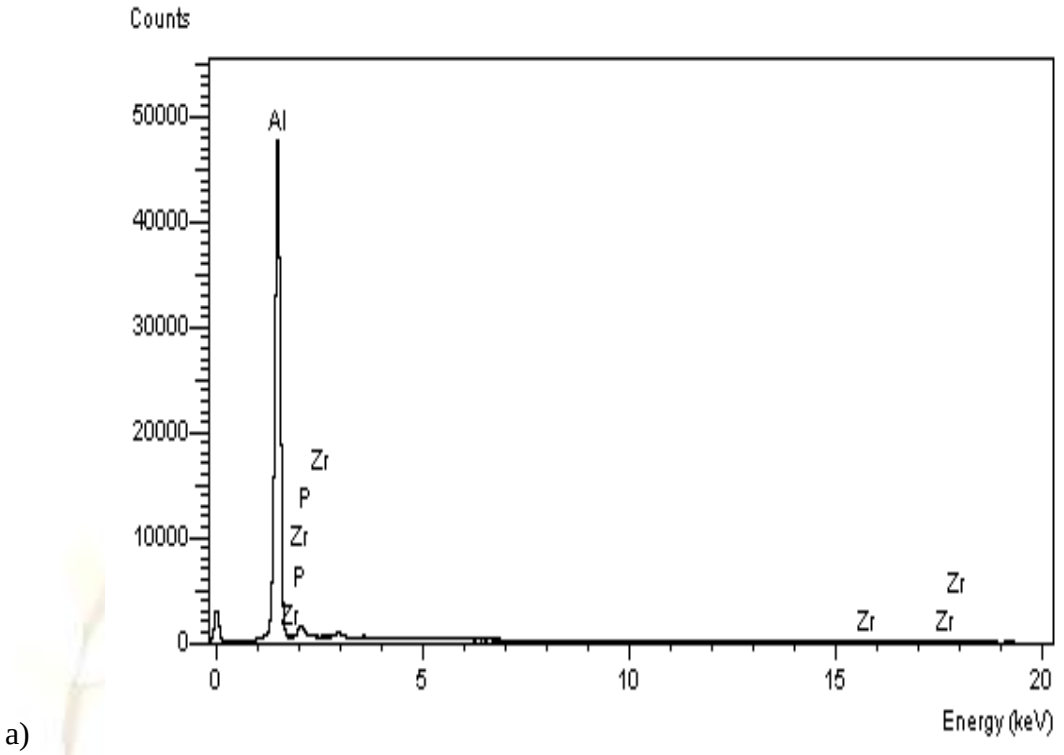

a)

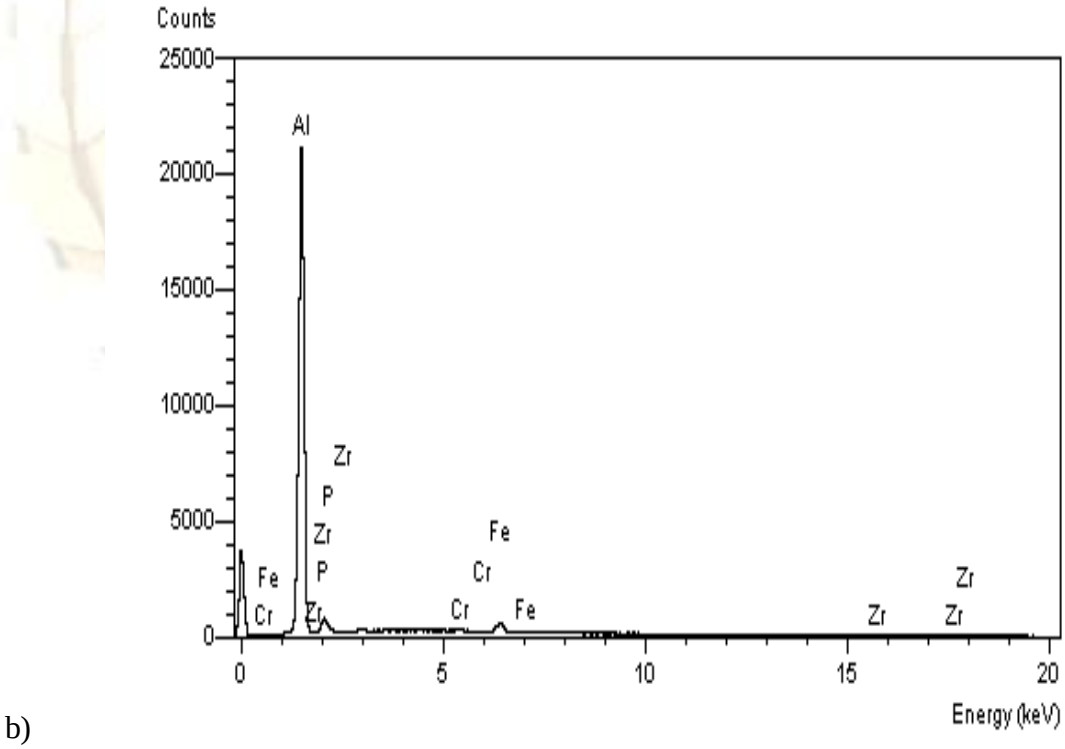

b)

Fig. 6 : EDS patterns of Al–Al_2O_3-ZrO_2 powders milled at 300rpm for 45 h: (a) Al–Al_2O_3-ZrO_2 mix without milling, (b) as-milled Al–Al_2O_3-ZrO_2 powders, milled at 300 rpm for 45 h.

3.4 TEM Analysis

Fig. 7 shows TEM picture of the Al–10% Al_2O_3-10% ZrO_2 nanocomposites powder milled at 300rpm for 45h. The crystallite size measurements were obtained using TEM observations in order to compare these results with results obtained from XRD analysis. The more commonly methods have been used to determine the grain size are XRD methods. Sample preparation for XRD is simple and the resulted information is an average of a large number of grains. But for direct TEM, the results can be daunting, due to the time-consuming for sample preparation, the very small area investigated and the doubt about whether it is representative of the whole sample studied**.** Furthermore, it is possible to easily obtain the lattice strain data from the same analysis but it is more difficult by TEM methods. Fig. 7, shows that the crystallite size measurements were obtained using TEM observations are at range (21.7–25.3 nm).

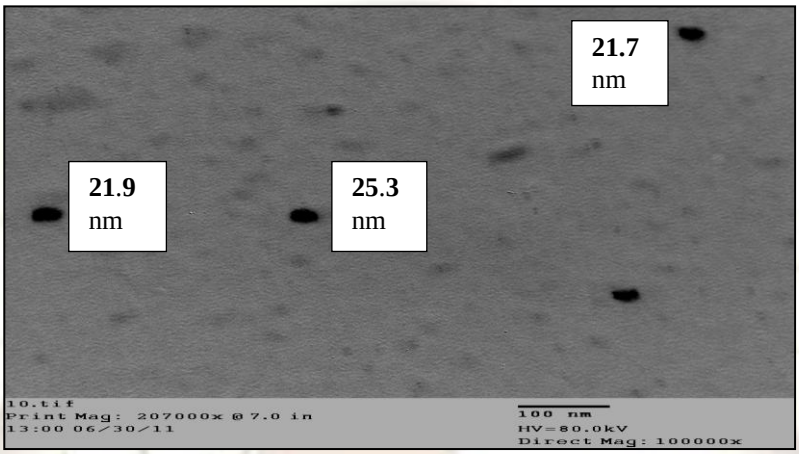

Fig. 7: TEM microstructure of Al–Al_2O_3-ZrO_2 powders milled at 300rpm for 45 h

3.5 Comparison between crystallite size measurements from XRD and TEM

Regarding the comparison between the results obtained from the Williamson–Hall method and direct TEM observations; Ungar [22] reviewed the meaning of size obtained from peak broadening in XRD patterns and compared these values with those obtained by direct microstructural studies, e.g., TEM. He pointed out that the two measurements can be: (1) identical to each other, (2), totally different or (3) in good qualitative correlation.

In this work the crystallite size value from WH method is 25.36 nm and from direct TEM is (21.7–25.3 nm). So, the grain sizes obtained by Williamson–Hall method and direct TEM observations are nearly the same i.e. they are in agreement with Ungar observations. Suryanarayana, [21] reported that the grain sizes obtained by the X-ray peak broadening studies, after incorporating the appropriate corrections, and the direct TEM techniques are expected to be the same, and this is achieved in this work and also in other cases for different system [23-25].

IV. Conclusions

In the present study, nanosized powders of Al-10% Al_2O_3-10% ZrO_2 have been synthesized by high energy mechanical milling. A homogenous distribution of the (Al_2O_3-ZrO_2) reinforcements in the Al matrix was obtained. Characterization of the mechanically milled powders confirmed uniform distribution of the reinforcement phase. By using WH method, it has shown that crystallite size decrease with milling time to steady value of 25.36 nm. At the same time, the lattice strain increases to a value of 0.139%. The grain sizes measurements obtained by the X-ray peak broadening studies, and the direct TEM techniques are nearly the same. Advanced material of Al-Al_2O_3-ZrO_2 hybrid nanocomposite can be fabricated. We believe that this is the first study on such nanocomposite hybrid systems with expected new properties.

References

[1] Poirier, D.; Drew, R.A.; Trudeauc, M.L.; Gauvin, R."Fabrication and properties of mechanically milled alumina/aluminum nanocomposites". Materials Science and Engineering A, 527, (2010), 7605–7614.

[2] Razavi, H. Z.; Simchi, A.; Seyed Reihani, S.M. "Structural evolution during mechanical milling of nanometric and micrometric Al_2O_3 reinforced Al matrix composites". Mater Sci Eng A, (2006), 428, 159-168.

[3] Suryanarayana, C. "Synthesis of Nanocomposites by mechanical alloying". Journal of Alloys and Compounds, 509, supplement 1, (2011), S229-S234.

[4] Ozdemir I., Ahrens S., Mucklich S., Wielage B., "Nanocrystalline Al–Al_2O_3p and SiCp composites produced by high-energy ball

milling", journal of materials processing technology 205, (2008),111-118.

[5] Yadav, T. P., Yadav, R.M., Singh D.P. "Mechanical Milling: a Top Down approach for the Synthesis of Nanomaterials and Nanocomposites", Nanoscience and Nanotechnology, (2012), 2(3),

[6] Khadem, S.A.; Nategh,. S.; Yoozbashizadeh, H. "Structural and morphological evaluation of Al-5 vol.% SiC nanocomposite powder produced by mechanical milling", Journal of Alloys and Compounds, 2011, 509, 2221.

[7] Prabhu, B.; Suryanarayana, C.; An, L.; Vaidyanathan, R. "Synthesis and characterization of high volume fraction Al–Al_2O_3 nanocomposite powders by high-energy milling", Materials Science and Engineering A, (2006), 425, 192–200.

[8] Suryanarayana, C. "Mechanical alloying and milling". Prog. Mater. Sci., (2001), 46, 1-184.

[9] Mohana, B.; Rajadurai, A.; Satyanarayana, K.G. "Electric discharge machining of Al–SiC metal matrix composites using rotary tube electrode". J Mater Process Technol, (2004), 153:978.

[10] Gingua, O.; Mangraa, M.; Orban, R.L. "In-situ production of Al/SiCp composite by laser deposition Technology", J Mater Process Technol, (1999), 89:187.

[11] Cambronero, L.E.G.; Sa´nchez, E; Ruiz-Roman, J.M.; Ruiz-Prieto, J.M. "Mechanical characterization of AA7015 aluminum alloy reinforced with ceramics", J Mat. Process Technol, (2003), 378, 143–144.

[12] Zebarjad, S.M.; Sajjadi, S.A. "Microstructure evaluation of Al–Al_2O_3 composite produced by mechanical alloying method", Mater Des, (2006), 27:684.

[13] Bandyopadhyy A.K., "Nano Materials", New Age International publishers, second editon (2010).

[14] Langford JI. ," A rapid method for analyzing the breadths of diffraction and spectral lines using Voigt function", J Appl Crystallogr 11, (1978), 10–4,

[15] Williamson K. G., Hall H. W., "X-ray broadening from field aluminium and wolfram", Acta Metall. Metall,; (1953), 1:22,.

[16]. Rebhi, A., Makhlouf, T., Njah, N.,"X-Ray diffraction analysis of 99.1% recycled Al subjected to equal channel angular extrusion", Physics Procedia 2, (2009), 1263-1270.

[17] Mhadhbi M., Khitouni M., Azabou M., Kolsi A. "Characterization of Al and Fe nanosized powders synthesized by high energy mechanical milling" Materials Characterization 59, (2008), 944-950,.

[18] Daly, R.; Khitouni, M.; Kolsi, A. W.; Njah, N. "The studies of crystallite size and microstrains in aluminum powder prepared by mechanical milling" physica status solidi (c) vol. 3 issue 9 , (2006), 3325 – 3331.

[19] Azabou M., Khitouni M., Kolsi A. "Characterization of nanocrystalline Al-based alloy produced by mechanical milling followed by cold-pressing consolidation" Materials Characterization 60,(2009), 499-505.

[20] Mahboob H, Sajjadi S. A., Zebarjad S. M. "Synthesis of Al-Al_2O_3 Nano-composite by Mechanical Alloying and evaluation of the effect of ball Milling time on the microstructure and mechanical Properties" the Int. Conf. on MEMS and Nanotechnology (Kuala Lumpur-Malaysia) ICMN 8, (2008), 13-15.

[21] Suryanarayana, C. "Mechanical Alloying and Milling", Marcel Dekker, Inc., New York, NY,(2004)

[22] Ungar, T.," The meaning of size obtained from broadened X-ray diffraction peaks", Adv. Eng. Mater. 5: (2003), 323–329,.

[23] Tsuzuki, T., McCormick, P.G.," Synthesis of metal oxide nanoparticles by mechano chemical process" sing. Mater. Sci. Forum (2000) , 343–346 , 383–388.

[24] Liu,K.W.,Mucklich, F., Pitschke, W., Birringer, R., Wetzig, K. "Synthesis of nanocrystalline B_2 structured (Ru, Ir) Al in the ternary Ru-Al-Ir system by mechanical alloying and its thermal stability". Z. Metallkde, 92:924–930, (2001).

[25] Ahn, J. H., Wang, G. X., Liu, H. K., Dou, S. X. "Mechanically Milled Nanocrystalline Ni_3Sn_4 and $FeSi_2$ Alloys as an Anode Material for Li-Ion Batteries", Mater. Sci. For.360–362: (2001), 595–602,

List of Figures